NASA Technical Memorandum 88276

Thermal Stress Analysis of Space Shuttle Orbiter Wing Skin Panel and Thermal Protection System

William L. Ko and Jerald M. Jenkins

March 1987

National Aeronautics and
Space Administration

NASA Technical Memorandum 88276

Thermal Stress Analysis of Space Shuttle Orbiter Wing Skin Panel and Thermal Protection System

William L. Ko and Jerald M. Jenkins
Ames Research Center, Dryden Flight Research Facility, Edwards, California

1987

National Aeronautics and
Space Administration
Ames Research Center
Dryden Flight Research Facility
Edwards, California 93523-5000

SUMMARY

Preflight thermal stress analysis of the space shuttle orbiter wing skin panel and the thermal protection system (TPS) was performed. The heated skin panel analyzed was rectangular in shape and contained a small square cool region at its center. The wing skin immediately outside the cool region was found to be close to the state of elastic instability in the chordwise direction based on the conservative temperature distribution. The wing skin was found to be quite stable in the spanwise direction. The potential wing skin thermal instability was not severe enough to tear apart the strain isolation pad (SIP) layer.

Also, the preflight thermal stress analysis was performed on the TPS tile under the most severe temperature gradient during the simulated reentry heating. The tensile thermal stress induced in the TPS tile was found to be much lower than the tensile strength of the TPS material. The thermal bending of the TPS tile was not severe enough to cause tearing of the SIP layer.

INTRODUCTION

The space shuttle orbiter reenters the earth's atmosphere at extremely high velocity (almost Mach 25 at the reentry altitude of 400,000 ft). Because of severe reentry aerodynamic heating encountered by the shuttle orbiter, the entire shuttle structure is covered with a thermal protection system (TPS).

Three types of TPS are used to protect the orbiter: (1) felt reusable surface insulation (FRSI), (2) low-temperature reusable surface insulation (LRSI), and (3) high-temperature reusable surface insulation (HRSI). The FRSI is a highly flexible blanket-type layer of heat shield, which is bonded to the low-heating zones of the orbiter (for example, the wing upper surface and the outer surface of the payload bay door) with room-temperature vulcanized (RTV) rubber. The LRSI (white tiles) and HRSI (black tiles) are the low-density porous silica tiles. Each tile, which has an average size of 6 in by 6 in, is individually bonded with RTV rubber to the orbiter structure with a strain isolation pad (SIP) layer sandwiched in between. The SIP layer is highly flexible and serves as a cushion to absorb the thermal strain incompatibility between the TPS tiles and the aluminum skins. The LRSI is used in the medium heating zones, such as the upper region of the glove and the wing upper surface near the leading edges. The HRSI is used in the highly heated areas, such as the lower surfaces of the wings and fuselage. Some of the gaps between the TPS tiles in the highly heated areas are filled with ceramic-coated alumina mats (gap fillers) to prevent hot gases from coming in contact with the substructure at the bottom of the gaps.

Before the first space transportation system (STS) flight of the space shuttle orbiter Columbia, all possible critical structural problems induced by the reentry heating had to be investigated. One concern was the possible thermal buckling of the orbiter skin panels. Although the SIP layer is designed to absorb the possible skin buckling effect on the TPS tiles, in case the skin buckling is too severe, the TPS tiles might debond from the skin, causing a partial or total loss of the TPS function.

Another concern before the STS flights was the possible loss of the TPS tiles during the forced convective cooling period after the end of the reentry heating when the structural temperatures have reached their peak values. At this time, if some TPS tiles should detach from the skin and cause the skin to be exposed to the outside cool air, the thermal gradient buildup in the skin might cause an elastic instability in this region and cause more TPS tiles to detach from the skin.

Another key concern was the effect of TPS thermal deformation on the SIP layer. During the reentry when the TPS is under the most severe thermal gradient, the resulting TPS thermal deformation might pull the SIP layer apart and cause debonding of the TPS.

The purpose of this report is to perform the analysis on these potential problems and to draw some preliminary conclusions on the severity of their effects.

NOMENCLATURE

CQUAD2	NASTRAN quadrilateral membrane and bending element
c	one-half of TPS thickness, in
D	flexural rigidity of aluminum plate, $\frac{E_a t^3}{12(1-\nu_a^2)}$, in-lb
E	elliptic function of the second kind
E_a	modulus of elasticity of aluminum material, lb/in^2
E_s	modulus of elasticity of SIP, lb/in^2
E_T	modulus of elasticity of TPS, lb/in^2
FRSI	felt reusable surface insulation
HRSI	high-temperature reusable surface insulation
h	peak deflection at center of rectangular panel, in
k	modulus of elliptic function
L	one-half of TPS length (or width), in
LRSI	low-temperature reusable surface insulation
ℓ	width of rectangular panel, in
M_T	bending moment induced by thermal stresses in TPS, in-lb
m	number of buckled half-waves in x-direction

N_x	panel compressive load, lb/in
n	number of buckled half-waves in y-direction
p	length of rectangular panel, in
$\bar{p}$	deformed length of p, in
RTV	room-temperature vulcanized (rubber)
SIP	strain isolation pad
STS	space transportation system
T	temperature, °F
T_a	average temperature across TPS thickness, °F
TPS	thermal protection system
t	thickness of aluminum skin panel, in
t_s	thickness of SIP layer, in
w	lateral deflection of rectangular plate element
x, y, z	rectangular Cartesian coordinates
x_o	chordwise station
y_o	spanwise station
α_T	coefficient of thermal expansion of TPS, in/in-°F
ϵ_x	strain in x-direction, in/in
ϵ_s	strain in SIP thickness direction, in/in
ν_a	Poisson's ratio of aluminum material
ν_T	Poisson's ratio of TPS material
σ_c	magnitude of peak compressive stress in SIP thickness direction induced by TPS deformation, lb/in^2
σ_f	tensile strength of TPS, lb/in^2
σ_s	maximum stress in SIP thickness direction induced by aluminum skin buckling, lb/in^2

σ_t peak tensile stress in SIP thickness direction induced by TPS deformation, lb/in^2

σ_x, σ_y stresses in x- and y-directions, respectively, in aluminum panel or in TPS, lb/in^2

σ_z stress in SIP thickness direction induced by TPS deformation, lb/in^2

ϕ $\frac{\pi x}{p}$

Subscript:

cr value at buckling

DESCRIPTION OF WING SKIN PANEL

Figure 1 shows the location of the space shuttle orbiter left wing lower skin panel that was investigated. The rectangular skin panel is bounded by stations x_o1249 and x_o1307 in the chordwise direction, and by stations y_o-226 and y_o-254 in the spanwise direction. The reinforcing hat stringers are oriented in the spanwise direction. Figure 2 shows an enlarged view of the rectangular panel. Consider that the panel has been heated up to a peak temperature of 320°F (the estimated worst case of heating) near the end of reentry. Suppose one TPS tile (6 in by 6 in) located in the center region of the panel is lost after the simulated reentry heating and causes the wing skin in the central region of the 6-in by 6-in area to be cooled down to some lower temperature, say, 180°F, by the outside cool air. The resulting thermal gradient buildup might induce thermal buckling in the periphery of the cooled region (fig. 2). The problem is to calculate the induced thermal stresses in the panel, to estimate the degree of severity of the possible thermal buckling, and to explore if the skin buckling will cause the TPS tiles adjacent to the cooled region to debond from the wing skin.

THERMAL STRESS ANALYSIS

A NASA structural analysis (NASTRAN) finite-element computer program (refs. 1 and 2) was used in the thermal stress analysis of the orbiter wing skin panel. In setting up the NASTRAN structural model (fig. 3), the hat-stringer reinforced skin panel was replaced with an equivalent panel of uniform effective thickness. The model has 117 grid points and 96 quadrilateral membrane and bending elements (CQUAD2, refs. 1 and 2). The cool and hot regions were maintained at constant temperatures of 180°F and 320°F, respectively. The boundary conditions used were (1) free edges and (2) fixed edges.

Figure 4 shows distributions of thermal stress $\sigma_y(x)$ along the x-axis predicted from the NASTRAN. The solid stepped curve is for the free edges; the dashed stepped curve is for the fixed edges. The peak compressive stress near the boundary of the

cool region for the case of free edges is $\sigma_y(x) = 5140$ lb/in^2. The cool region is under considerable tension. If the NASTRAN elements were refined, the value of the peak compressive stress might become larger. Figure 5 shows the distributions of thermal stress $\sigma_x(y)$ along the y-axis calculated from the NASTRAN. The stepped solid and dashed curves are for the free and the fixed edges, respectively. For the free-edge condition, the NASTRAN gives $\sigma_x(y) = 4960$ lb/in^2 for the peak compressive stress near the boundary of the cool region. Again, refinement of the NASTRAN elements may increase the value of the peak compressive stress.

BUCKLING ANALYSIS

After the peak values of the compressive stresses near the boundary of the cool region are known, the next problem to consider is the possible buckling of the skin panel element immediately outside the cool region.

Consider a small rectangular skin element 1 (fig. 6) of length p and width ℓ, located between the two adjacent hat stringers and in the highly compressed region (the immediate exterior of the cool region). For simplicity, the deformed shape of the rectangular element may be assumed to be

$$w = h \sin \frac{\pi x}{p} \sin \frac{\pi y}{\ell} \tag{1}$$

where w is the deflection of the rectangular plate element and h is its peak value at the center of the rectangular plate element. Based on this deformed shape, the buckling load $(N_x)_{cr}$ for a simply supported rectangular plate uniformly compressed in the x-direction may be expressed as (taking m = n = 1, ref. 3)

$$(N_x)_{cr} = \frac{\pi^2 D}{p^2} \left(1 + \frac{p^2}{\ell^2}\right)^2 \tag{2}$$

where m and n are the numbers of half-waves in the x- and y-directions, respectively, and D is given by

$$D \equiv \frac{E_a t^3}{12(1 - \nu_a^2)} \tag{3}$$

where E_a is the modulus of elasticity of the aluminum material and t is the thickness of the element. Combining equations (2) and (3), the buckling stress $(\sigma_x)_{cr}$ may be expressed as

$$(\sigma_x)_{cr} = \frac{(N_x)_{cr}}{t} = \frac{\pi^2 E_a}{12(1 - \nu_a^2)} \frac{t^2}{p^2} \left(1 + \frac{p^2}{\ell^2}\right)^2 \tag{4}$$

where ν_a is Poisson's ratio of the aluminum material.

For the shuttle skin, t = 0.062 in and p = 1.75 in. Taking $E_a = 10 \times 10^6$ lb/in^2, $\nu_a = 0.33$, and $\ell = 2$ in, equation (4) yields

$$(\sigma_x)_{cr} = 3612 \text{ lb/in}^2 \tag{5}$$

This value lies between the two peak compressive stresses $\sigma_x = 2650$ lb/in^2 for the fixed-edge condition and $\sigma_x = 4960$ lb/in^2 for the free-edge condition (fig. 5). If the actual edge condition is close to the free-edge condition, then the skin panel immediately outside the cool region is close to an elastic instability in the x-direction.

Next, consider the second rectangular skin element 2 (fig. 6), located between the two adjacent hat stringers next to the boundary of the cool region. For this case, the length of the plate is 6 in and the width is 1.75 in. Using equation (4) and replacing $(\sigma_x)_{cr}$, p, and ℓ, respectively, with $(\sigma_y)_{cr}$, 6 in, and 1.75 in, then $(\sigma_y)_{cr}$ may be calculated as

$$(\sigma_y)_{cr} = 169{,}340 \text{ lb/in}^2 \tag{6}$$

This value is many times greater than the peak compressive stress σ_y predicted from the NASTRAN (fig. 4) and indicates that no buckling will occur in the direction of the hat stringers.

Deflection Curve

As shown above, the wing skin near the boundary of the cool region could buckle in the x-direction (chordwise direction). The next problem is to calculate the panel peak deflection h (fig. 6) and to determine if h will cause debonding between the TPS tile and the SIP layer.

Based on equation (1), the deflection curve of the rectangular skin element in the $y = \frac{\ell}{2}$ plane may be written as (fig. 6)

$$w = h \sin \frac{\pi x}{p} \tag{7}$$

From equation (7), the slope of the deflection curve is given by

$$\frac{dw}{dx} = \frac{\pi h}{p} \cos \frac{\pi x}{p} \tag{8}$$

The small element of the curve length $d\bar{p}$ along the above deflection curve may be expressed as

$$d\bar{p} = \sqrt{1 + \left(\frac{dw}{dx}\right)^2}\, dx \tag{9}$$

Combining equations (8) and (9), the total curve length $\bar{p}$ of the deflection curve may be expressed as

$$\bar{p} = \int_0^p \sqrt{1 + \left(\frac{\pi h}{p}\right)^2 \cos^2 \frac{\pi x}{p}}\ dx \tag{10}$$

which may be expressed in terms of an elliptic function as (see appendix)

$$\frac{\bar{p}}{p} = \frac{2}{\pi} \sqrt{1 + \left(\frac{\pi h}{p}\right)^2}\ E\left(k, \frac{\pi}{2}\right) \tag{11}$$

where $E\left(k, \frac{\pi}{2}\right)$ is the complete elliptic integral of the second kind, and k is the modulus of the elliptic function given by

$$k \equiv \frac{1}{1 + \left(\frac{p}{\pi h}\right)^2} \tag{12}$$

As h << p, the integrand of equation (10) may be expanded and integrated as (see appendix)

$$\frac{\bar{p}}{p} = 1 + \frac{1}{4}\left(\frac{\pi h}{p}\right)^2 + \cdots \tag{13}$$

from which h may be expressed as

$$\frac{h}{p} \approx \frac{2}{\pi} \varepsilon_x \tag{14}$$

or

$$\frac{h}{p} \approx \frac{2}{\pi} \sqrt{\frac{\bar{p}}{p} - 1} = \frac{2}{\pi} \sqrt{\frac{\sigma_x}{E_a}} \tag{15}$$

Taking p = 1.75 in, $E_a = 10 \times 10^6$ lb/in^2, and $\sigma_x \approx 4960$ lb/in^2 (the peak compressive stresses predicted from NASTRAN for free edges, shown in figure 3), the value of h may be calculated from equation (15) to yield

$$h = 0.0248 \text{ in} \tag{16}$$

Stress Induced in SIP

After the deformation of the skin panel is known, the next problem to consider is whether the above skin deformation h could overstress the SIP layer. The thick-

ness t_s of the SIP layer is 0.16 in. Thus, the maximum strain ε_s in the SIP thickness direction induced by the skin buckling is

$$\varepsilon_s = \frac{h}{t_s} = \frac{0.0248}{0.16} = 0.1550 \text{ in/in} \tag{17}$$

From reference 4, the modulus of elasticity E_s for the SIP material is $E_s \approx 117$ lb/in^2. Therefore, the induced stress σ_s in the SIP thickness direction is

$$\sigma_s = E_s\varepsilon_s = 117 \times 0.1550 = 18.14 \text{ lb/in}^2 \tag{18}$$

This value is considerably lower than 40 lb/in^2, the tensile strength of the SIP material (ref. 4). It is therefore unlikely that the skin buckling will cause tearing of the SIP layer. The next problem that must be considered is the thermal interaction between the TPS and the SIP layer.

THERMAL INTERACTION BETWEEN TPS AND SIP

When the outer surface of the TPS is heated to high temperature during reentry, the TPS will deform due to a severe thermal gradient across its thickness. The problem is to calculate the thermal stresses generated in the TPS and to determine whether or not the TPS deformation will tear apart the SIP layer.

Thermal Stresses in TPS

Figure 7 shows the temperature distribution across the thickness of a TPS tile at 450 sec after simulated reentry, when the temperature gradient reaches the maximum value. The temperature curve shown in figure 7 was obtained from a one-dimensional heat-transfer analysis using simulated aerodynamic heating for the STS-1 flight trajectory (refs. 5 to 8). This temperature distribution will cause the TPS to deform and induce a stress distribution in the thickness direction of the SIP, as shown in figure 8. Assuming that the temperature distribution in the TPS is a function of z only (fig. 7) and neglecting the low shear resistance of SIP, the thermal stresses in the TPS in the x- and y-directions, σ_x and σ_y, may be written as

$$\sigma_x(z) = \sigma_y(z) = -\frac{\alpha_T E_T}{1 - \nu_T}[T(z) - T_a] \tag{19}$$

where α_T is the coefficient of thermal expansion of the TPS material, E_T is the modulus of elasticity of the TPS, ν_T is Poisson's ratio of the TPS, the quantity $\frac{\alpha_T E_T}{1 - \nu_T}$ is associated with biaxial deformation of the TPS tile in the x- and y-

directions, T(z) is the temperature at any point z in the TPS tile, and T_a is the average TPS temperature across its thickness (fig. 8) and is given by

$$T_a = \frac{1}{2c} \int_{-c}^{c} T(z)\, dz \tag{20}$$

where 2c is the thickness of the TPS tile.

The temperature curve shown in figure 7 may be represented by the following quadratic function of z:

$$T(z) = a_1 z^2 + a_2 z + a_3 \tag{21}$$

where the coefficients a_1, a_2, and a_3 are given by $a_1 = 609.58°F/in^2$, $a_2 = 946°F/in$, and $a_3 = 446.42°F$.

Based on the temperature profile given in equation (21), equation (20) may be integrated as

$$T_a = \frac{a_1 c^3}{3} + a_3 \tag{22}$$

Substitution of equations (21) and (22) into equation (19) yields

$$\sigma_x(z) = \sigma_y(z) = -\frac{\alpha_T E_T}{1 - \nu_T} a_1 \left[\left(z^2 - \frac{c^2}{3} \right) + a_2 z \right] \tag{23}$$

The maximum tensile stress is located at the lower surface of the TPS tile and is given by setting z = -c in equation (23); hence,

$$\sigma_x(-c) = \sigma_y(-c) = \frac{\alpha_T E_T}{1 - \nu_T} \left(a_2 c - \frac{2 a_1 c^2}{3} \right) \tag{24}$$

For the TPS with a 9-lb/ft^3 weight density, the physical properties and dimensions (ref. 7) are as follows: the modulus of elasticity $E_T = 2.5 \times 10^4$ lb/in^2, Poisson's ratio $\nu_T = 0.16$, the coefficient of thermal expansion $\alpha_T = 3.3684 \times 10^{-7}$ in/in-°F, the tensile strength $\sigma_f = 21$ lb/in^2, the thickness 2c = 2.54 in, and the length 2L = 6 in. Using these data and the values given previously for a_1 and a_2, equation (24) gives the maximum tensile stress in the TPS as

$$\sigma_x(-c) = \sigma_y(-c) = 4.02 \text{ lb/in}^2 \tag{25}$$

This value is only 19 percent of the TPS tensile strength $\sigma_f = 21$ lb/in^2. Thus, the TPS thermal deformation will not induce tensile failure at its lower surface.

Stresses Induced in SIP

The bending moment M_T induced by the thermal stress $\sigma_x(z)$ in the TPS is given by

$$M_T = \int_{-c}^{c} \sigma_x(z) z \, dz \tag{26}$$

Substituting equation (23) into equation (24) and integrating results in

$$M_T = -\frac{2}{3}\left(\frac{\alpha_T E_T}{1 - \nu_T}\right) a_2 c^3 \tag{27}$$

This moment M_T must be balanced by the resisting moment generated by the nonuniform distribution of the normal stress σ_z in the SIP thickness direction (fig. 8). The center region of the SIP will be under tension, and the regions near the edge of the SIP will be under compression because the TPS will bow upward under reentry heating.

Let σ_z be expressed as a quadratic function of x:

$$\sigma_z(x) = b_1 x^2 + b_2 x + b_3 \tag{28}$$

From figure 8, the coefficients b_1, b_2, and b_3 can be determined as

$$b_1 = -\frac{\sigma_t + \sigma_c}{L^2} \tag{29}$$

$$b_2 = 0 \tag{30}$$

$$b_3 = \sigma_t \tag{31}$$

where σ_t and σ_c are, respectively, the magnitudes of the peak tensile stress and the peak compressive stress in the SIP thickness direction. Substituting equations (29) to (31) into equation (28) yields

$$\sigma_z(x) = -(\sigma_t + \sigma_c)\frac{x^2}{L^2} + \sigma_t \tag{32}$$

The two stresses σ_t and σ_c may now be determined from the balance of forces and the balance of moments. For the balance of forces,

$$\int_0^L \sigma_z(x) \, dx = 0 \tag{33}$$

For the balance of moments,

$$\int_0^L \sigma_z(x) x \, dx = M_T \tag{34}$$

From equations (32) to (34), σ_t and σ_c may be expressed as

$$\sigma_t = -\frac{4}{L^2} M_T \tag{35}$$

$$\sigma_c = 2\sigma_t \tag{36}$$

Substituting equation (27) into equation (35) yields

$$\sigma_t = \frac{8}{3}\left(\frac{\alpha_T E_T}{1 - \nu_T}\right)\frac{a_2 c^3}{L^2} \tag{37}$$

Using the previously given known data, equation (37) yields

$$\sigma_t = 15.58 \text{ lb/in}^2 \tag{38}$$

If the aluminum skin deforms in the opposite direction of the TPS (worst case), then the total tensile stress induced in the SIP will be

$$\sigma_s + \sigma_t = 18.14 + 15.58 = 33.72 \text{ lb/in}^2 \tag{39}$$

This value is 85 percent of the SIP tensile strength, 40 lb/in^2 (ref. 7). Thus, it is unlikely that the combined deformations of the aluminum skin panel and TPS will tear the SIP layer.

CONCLUSIONS

Preflight thermal stress analysis was performed on a heated space shuttle wing rectangular skin panel containing a square cool region at its center. The analysis showed that based on a conservative temperature distribution, the wing skin immediately outside the cool region was close to an elastic instability in the direction transverse to the hat stringers. However, the wing skin thermal deformation was found not to be severe enough to cause tearing of the strain isolation pad (SIP) layer.

A preflight thermal stress analysis was also conducted on the thermal protection system (TPS) tile subjected to the most severe simulated reentry heating. Based on this analysis, the thermal stress generated in the TPS tile will not cause it to fail in tension, and the combined thermal deformation of the wing skin and the TPS tile is unlikely to cause tearing apart of the SIP layer.

National Aeronautics and Space Administration
Ames Research Center
Dryden Flight Research Facility
Edwards, California, July 25, 1986

APPENDIX — INTEGRATION OF EQUATION (10)

Rewriting equation (10),

$$\bar{p} = \int_0^p \sqrt{1 + \left(\frac{\pi h}{p}\right)^2 \cos^2 \frac{\pi x}{p}}\, dx \tag{40}$$

The integration of this equation may be carried out as follows. Let

$$\phi = \frac{\pi x}{p} \tag{41}$$

Then, equation (40) becomes

$$\bar{p} = \frac{p}{\pi} \int_0^\pi \sqrt{1 + \left(\frac{\pi h}{p}\right)^2 (1 - \sin^2 \phi)}\, d\phi \tag{42}$$

$$= \frac{p}{\pi} \int_0^\pi \sqrt{\left[1 + \left(\frac{\pi h}{p}\right)^2\right] \left[1 - \frac{1}{1 + \left(\frac{p}{\pi h}\right)^2} \sin^2 \phi\right]}\, d\phi \tag{43}$$

$$= \frac{2p}{\pi} \sqrt{1 + \left(\frac{\pi h}{p}\right)^2} \int_0^{\pi/2} \sqrt{1 - k^2 \sin^2 \phi}\, d\phi \tag{44}$$

or

$$\frac{\bar{p}}{p} = \frac{2}{\pi} \sqrt{1 + \left(\frac{\pi h}{p}\right)^2}\, E\left(k, \frac{\pi}{2}\right) \tag{45}$$

where $E\left(k, \frac{\pi}{2}\right)$ is the complete elliptical integral of the second kind given by

$$E\left(k, \frac{\pi}{2}\right) = \int_0^{\pi/2} \sqrt{1 - k^2 \sin^2 \phi}\, d\phi \tag{46}$$

and k is defined as

$$k = \frac{1}{1 + \left(\frac{p}{\pi h}\right)^2} \tag{47}$$

Equation (45) is the equation (11).

Since h << p, the integrand of equation (40) may be expanded to give

$$\bar{p} = \int_0^p \left[1 + \frac{1}{2}\left(\frac{\pi h}{p}\right)^2 \cos^2 \frac{\pi x}{p} + \ldots\right] dx \tag{48}$$

Using equation (41), equation (48) may be written as

$$\bar{p} = \frac{p}{\pi} \int_0^\pi \left[1 + \frac{1}{2}\left(\frac{\pi h}{p}\right)^2 \cos^2 \phi + \ldots\right] d\phi \tag{49}$$

$$= \frac{p}{\pi}\left[\phi + \frac{1}{2}\left(\frac{\pi h}{p}\right)^2 \left(\frac{1}{2}\phi + \frac{1}{4}\sin^2 \phi\right) + \ldots\right]_0^\pi \tag{50}$$

$$= \frac{p}{\pi}\left[\pi + \frac{1}{4}\left(\frac{\pi h}{p}\right)^2 \pi + \ldots\right] \tag{51}$$

or

$$\frac{\bar{p}}{p} = 1 + \frac{1}{4}\left(\frac{\pi h}{p}\right)^2 + \ldots \tag{52}$$

which is equation (13).

REFERENCES

1. The NASTRAN® Theoretical Manual. NASA SP-221(05), Level 17.5, 1978.

2. The NASTRAN® User's Manual. NASA SP-222(05), Level 17.5, 1978.

3. Timoshenko, Stephen; and Gere, James M.: Theory of Elastic Stability. Second ed. McGraw-Hill Book Co., Inc., New York, 1961.

4. Sawyer, J.W.; and Rummler, D.R.: Room Temperature Mechanical Properties of Shuttle Thermal Protection System Materials. NASA TM-81786, 1980.

5. Ko, William L.; Quinn, Robert D.; Schuster, Lawrence S.; and Gonzales, David: Preflight Reentry Heat Transfer Analysis of Space Shuttle. AIAA-81-2382, Nov. 1981.

6. Ko. William L.; Quinn, Robert D.; and Gong, Leslie: Reentry Heat Transfer Analysis of the Space Shuttle Orbiter. Computational Aspects of Heat Transfer in Structures, H. M. Adelman, ed. NASA CP-2216, 1982, pp. 295-325.

7. Gong, Leslie; Quinn, Richard D.; and Ko, William L.: Reentry Heating Analysis of Space Shuttle With Comparison of Flight Data. Computational Aspects of Heat Transfer in Structures, H. M. Adelman, ed. NASA CP-2216, 1982, pp. 271-194.

8. Ko, William L.; Quinn, Robert D.; and Gong, Leslie: Finite-Element Reentry Heat-Transfer Analysis of Space Shuttle Orbiter. NASA TP-2657, 1986.

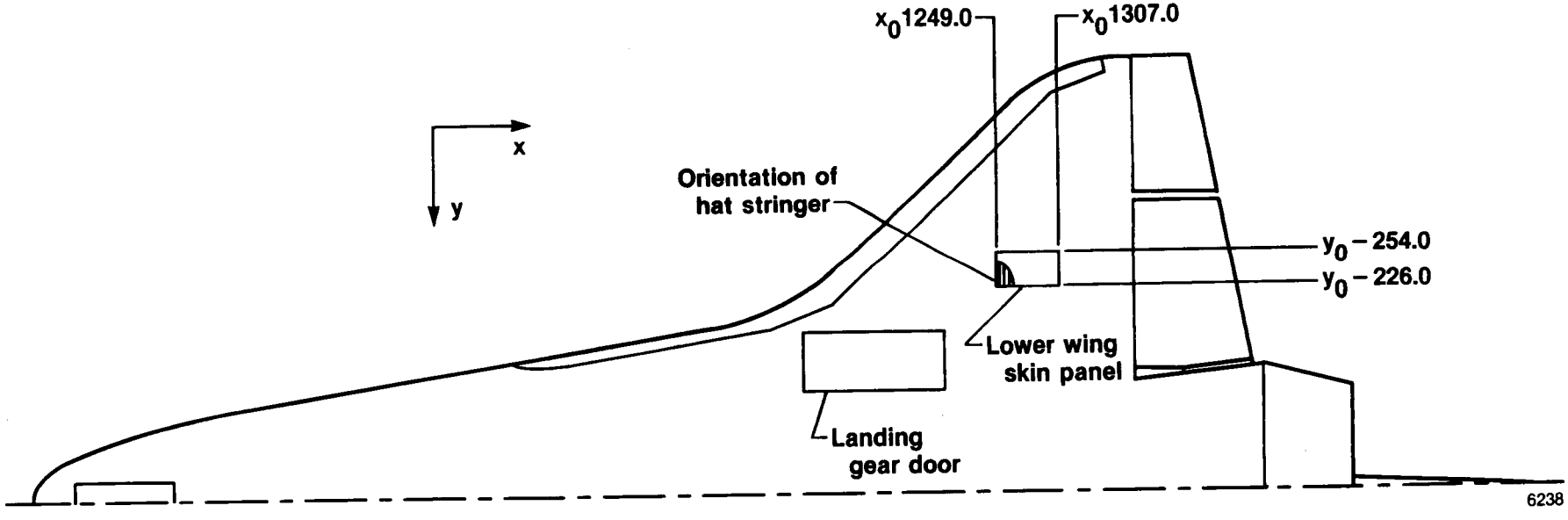

Figure 1. Location of skin panel on space shuttle orbiter left wing lower skin.

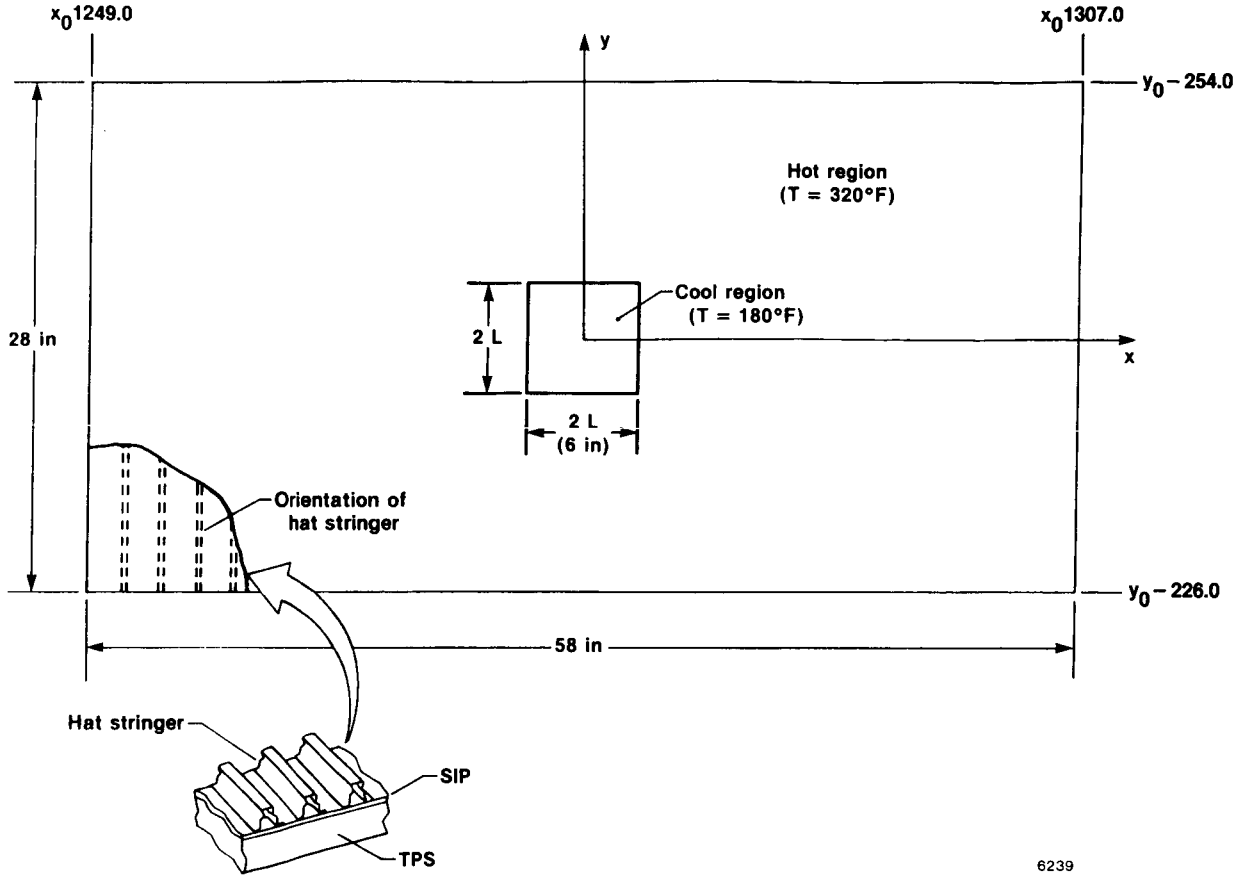

Figure 2. Geometry of skin panel.

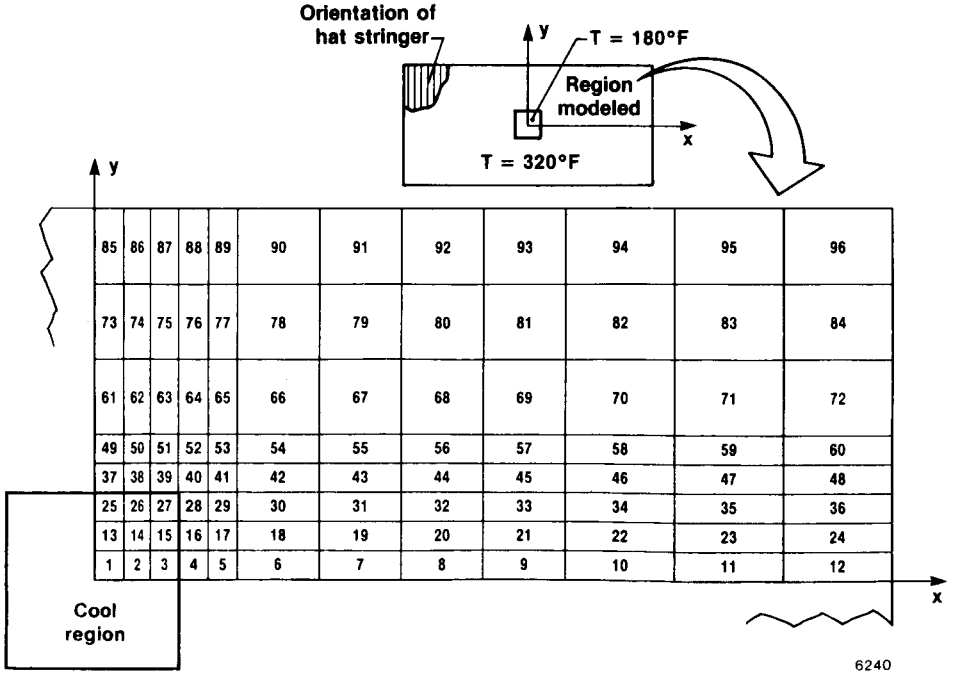

Figure 3. NASTRAN model of quarter skin panel.

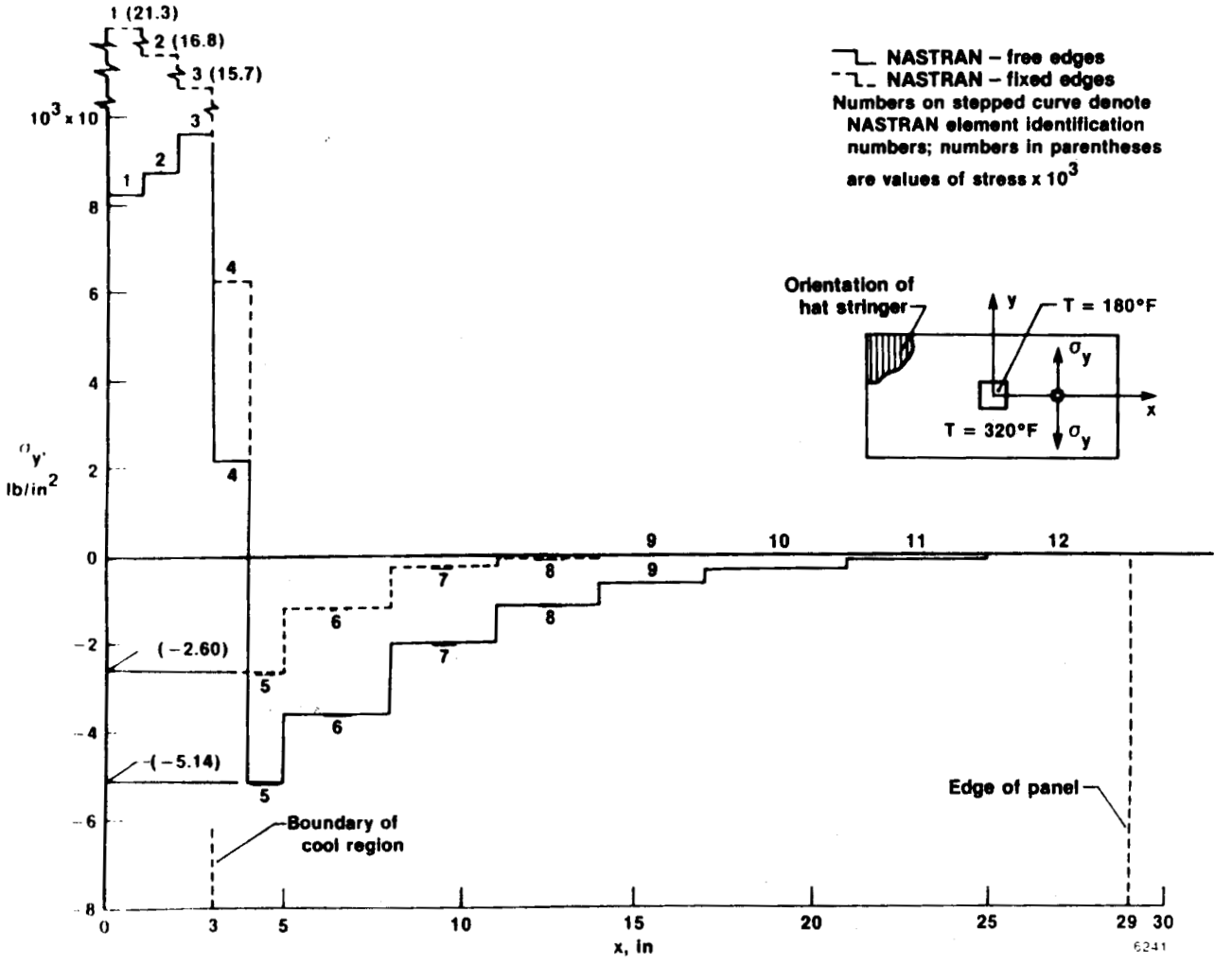

Figure 4. Distribution of σ_y along x-axis of skin panel.

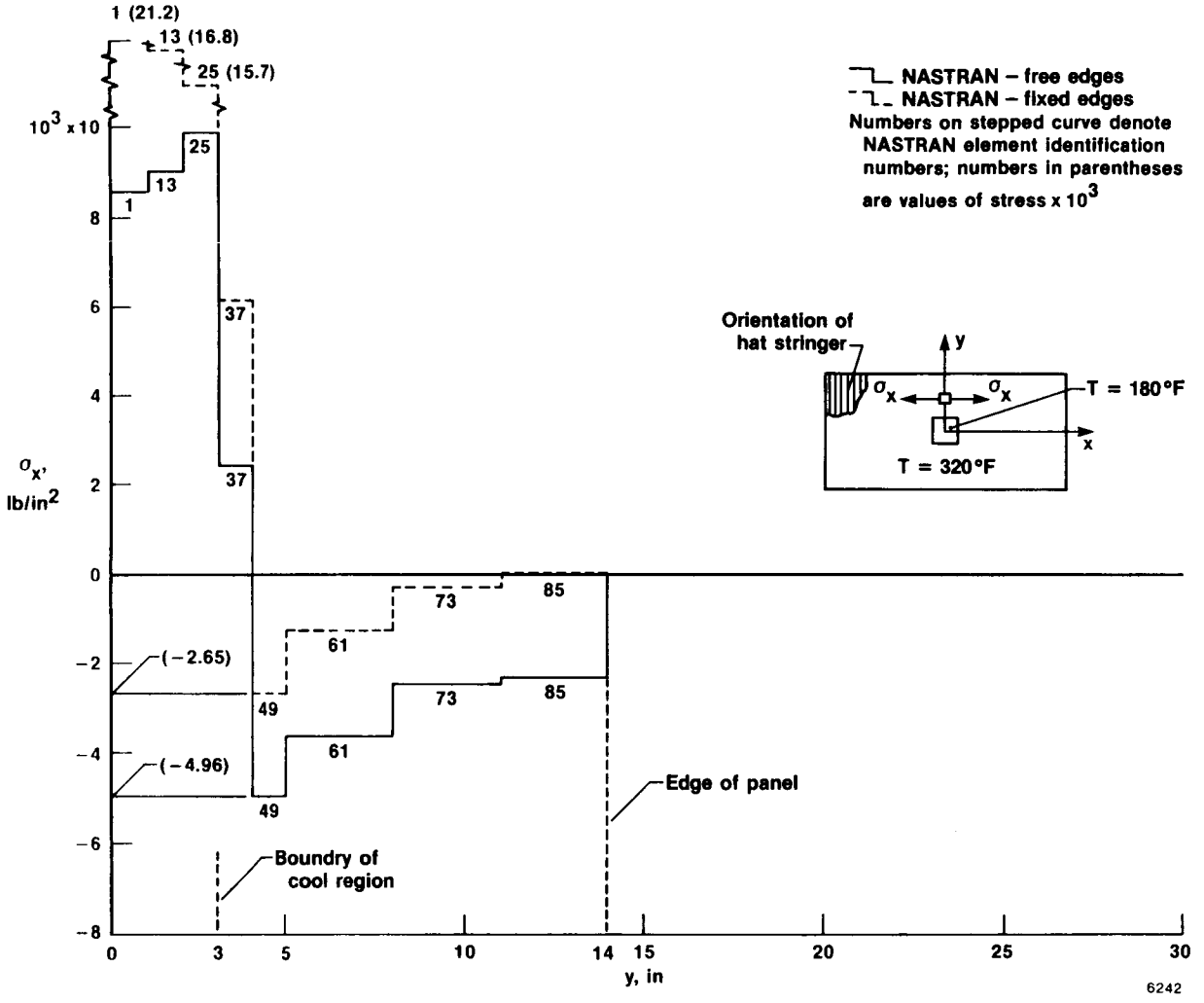

Figure 5. Distribution of σ_x along y-axis of skin panel.

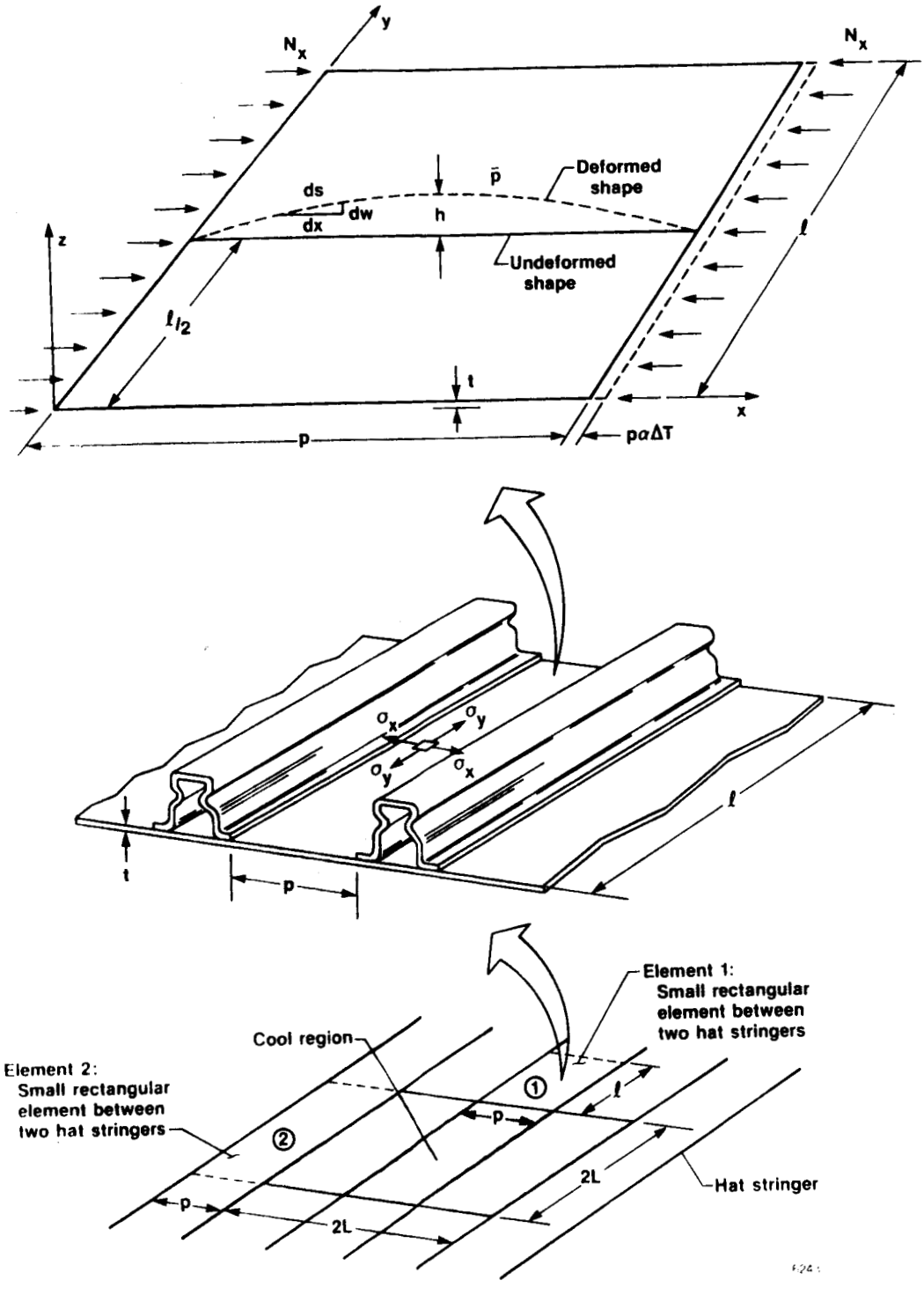

Figure 6. Thermal loadings of rectangular skin elements.

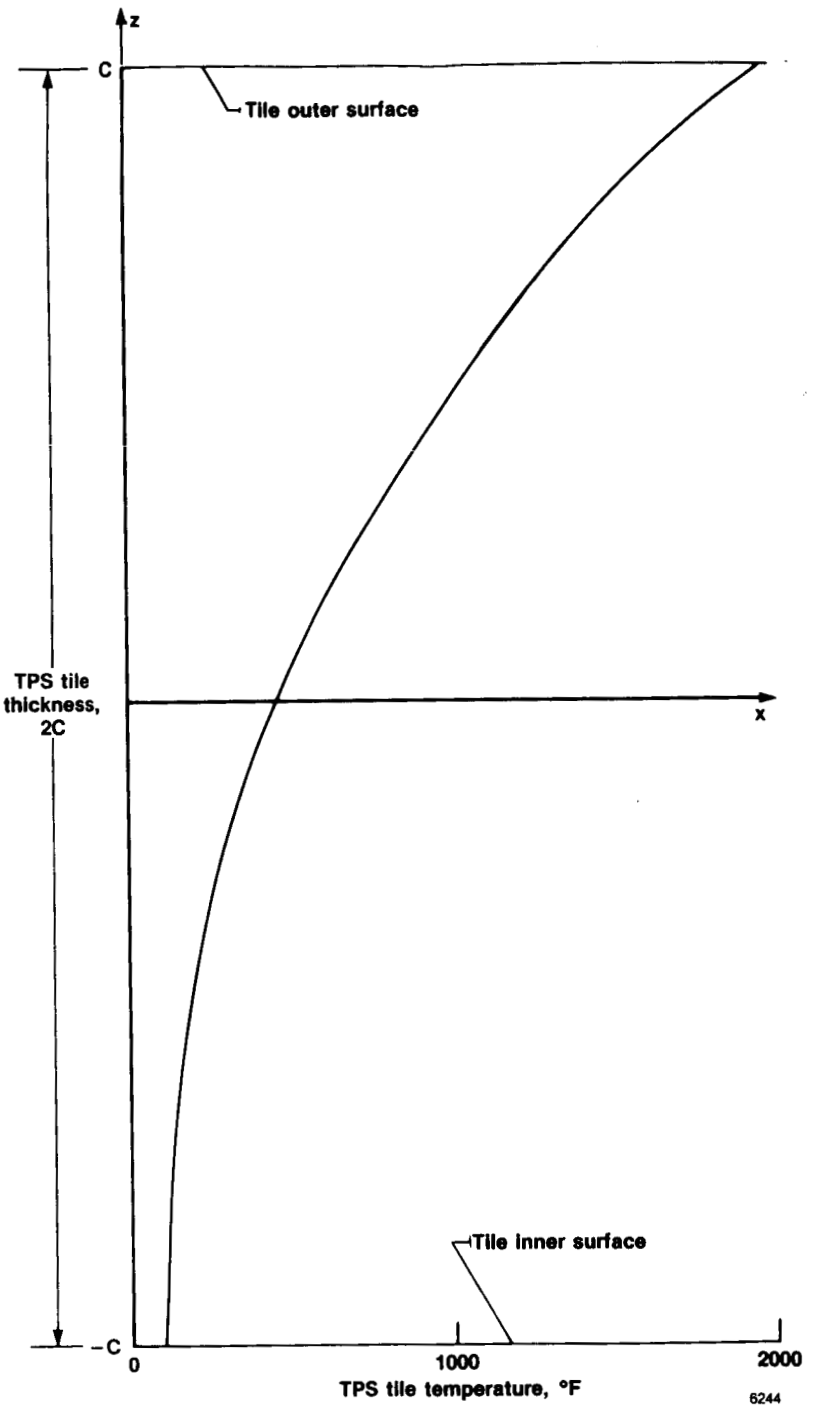

Figure 7. Calculated temperature distribution across thickness of TPS tile.

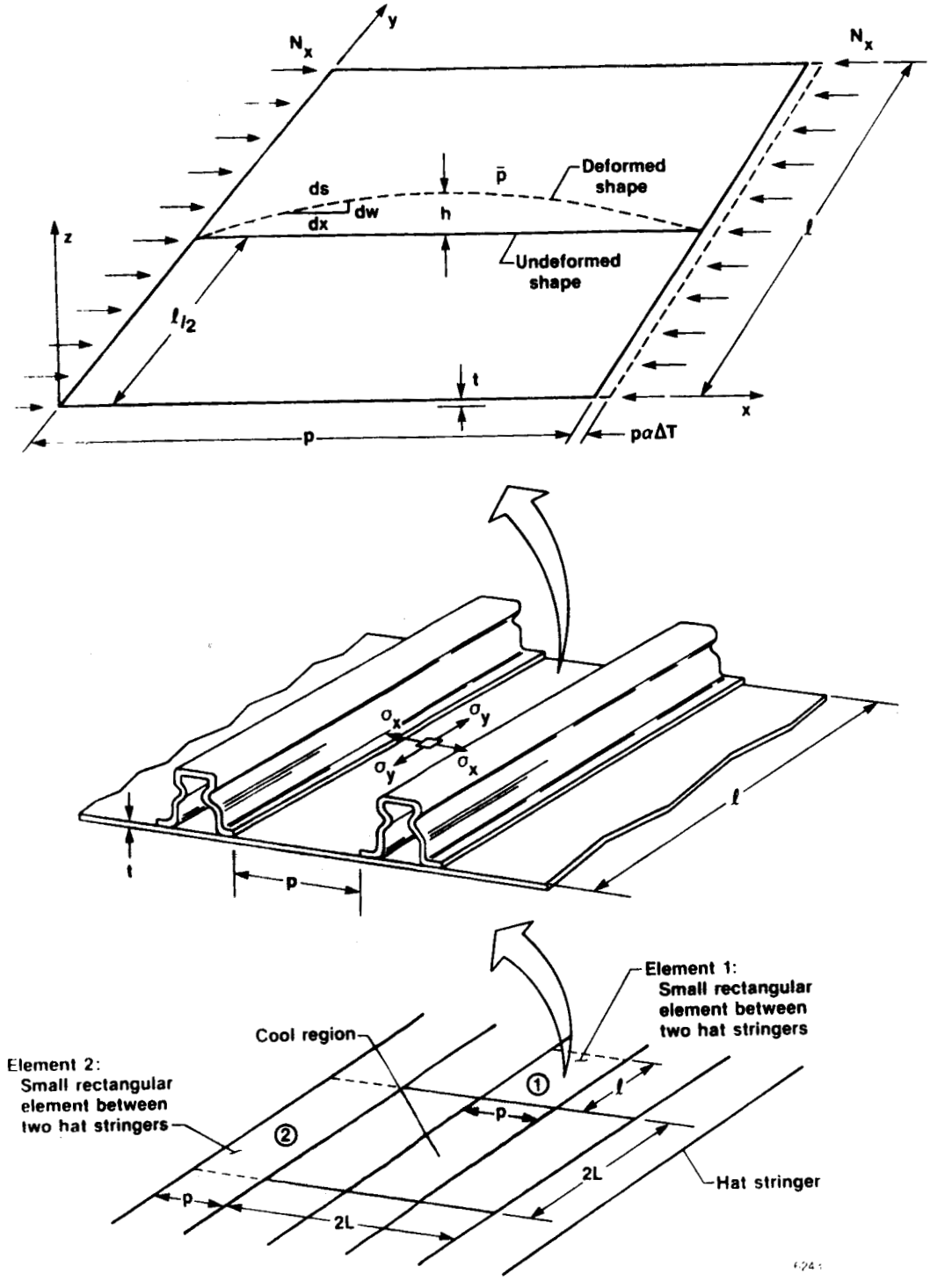

Figure 6. Thermal loadings of rectangular skin elements.

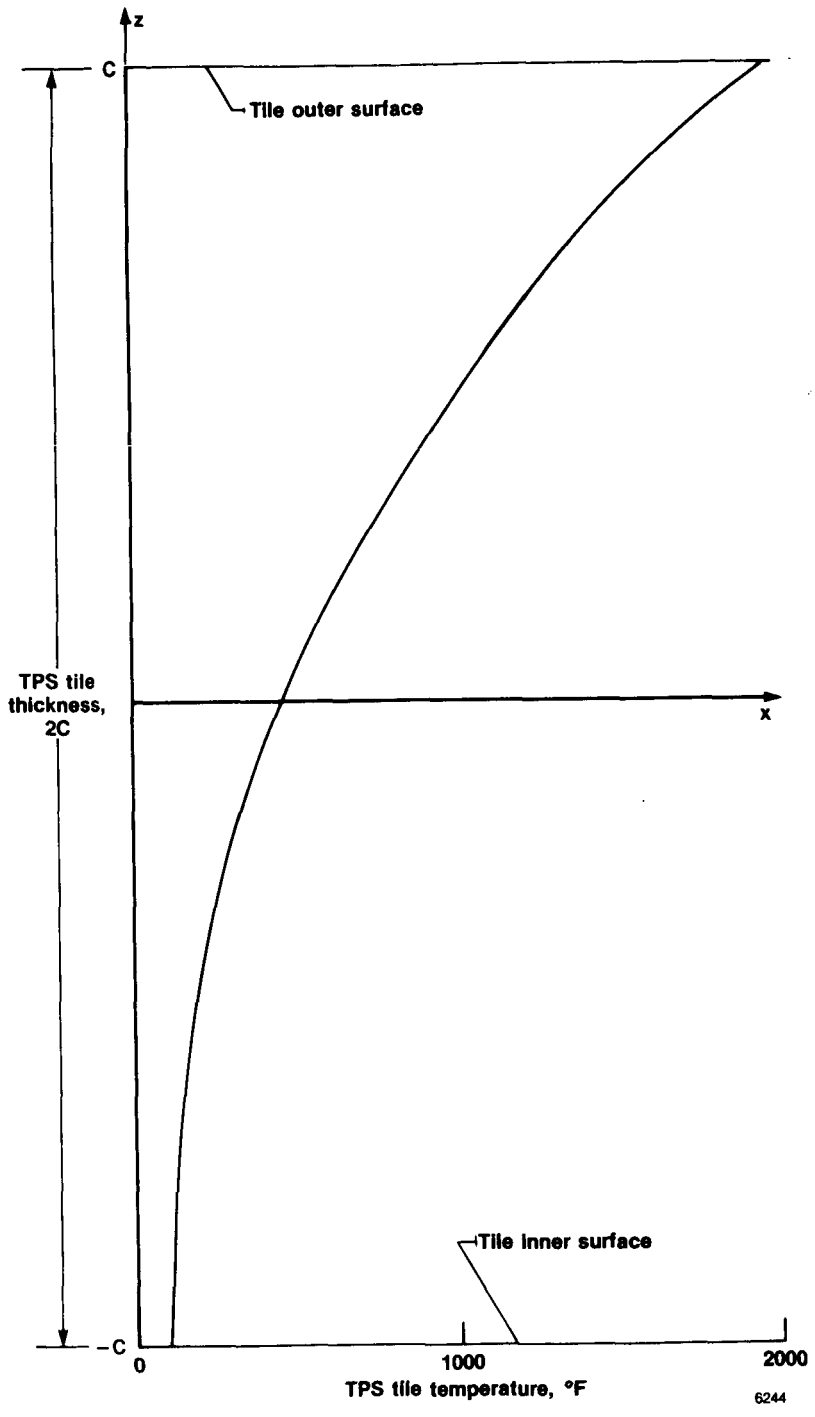

Figure 7. Calculated temperature distribution across thickness of TPS tile.

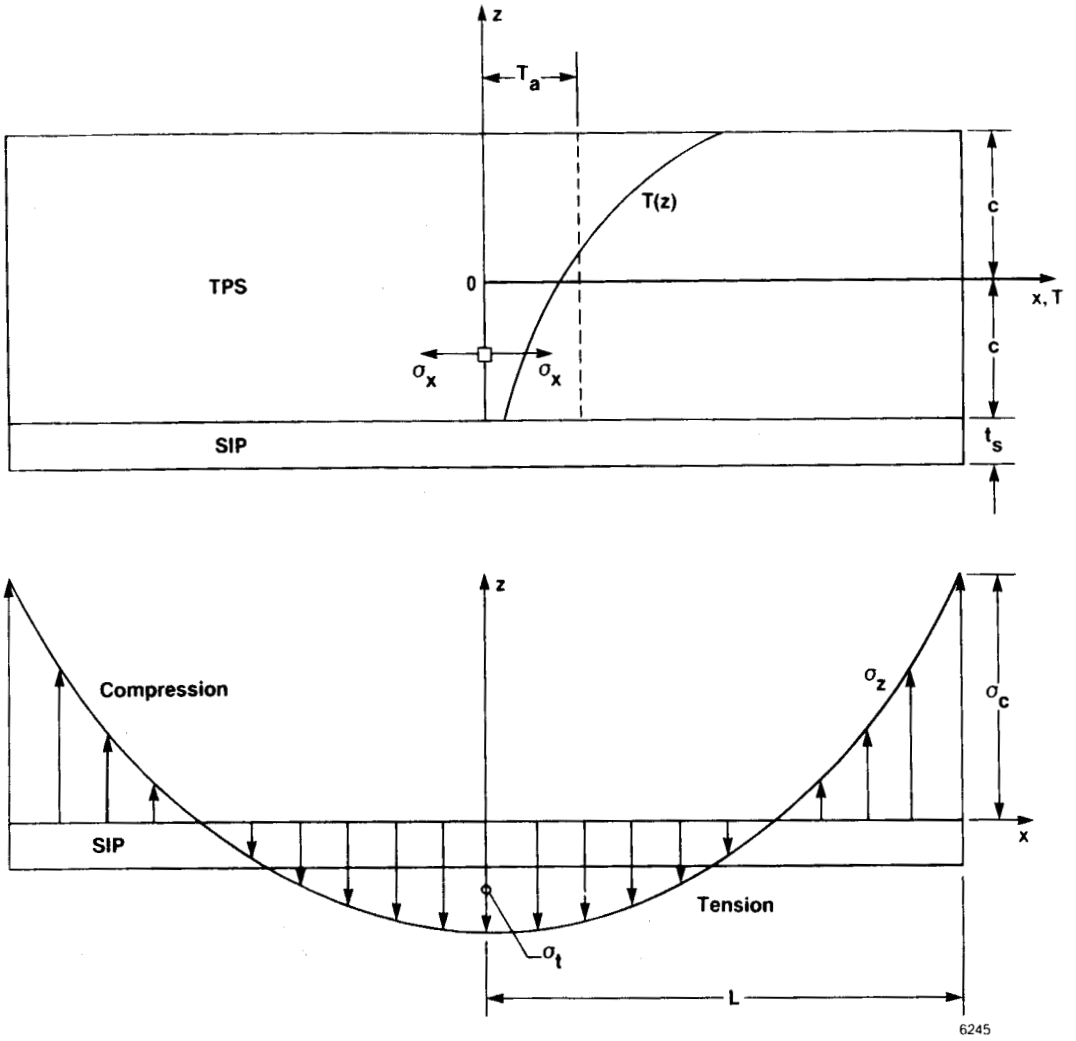

Figure 8. Stress distribution in SIP thickness direction induced by thermal deformation of TPS tile.

1. Report No.	2. Government Accession No.	3. Recipient's Catalog No.
NASA TM-88276		

4. Title and Subtitle	5. Report Date
Thermal Stress Analysis of Space Shuttle Orbiter Wing Skin Panel and Thermal Protection System	March 1987
	6. Performing Organization Code
7. Author(s)	8. Performing Organization Report No.
William L. Ko and Jerald M. Jenkins	H-1382
	10. Work Unit No.
9. Performing Organization Name and Address	RTOP 505-53-51
NASA Ames Research Center Dryden Flight Research Facility P.O. Box 273 Edwards, CA 93523-5000	11. Contract or Grant No.
	13. Type of Report and Period Covered
12. Sponsoring Agency Name and Address	Technical Memorandum
National Aeronautics and Space Administration Washington, DC 20546	14. Sponsoring Agency Code

15. Supplementary Notes

16. Abstract

Preflight thermal stress analysis of the space shuttle orbiter wing skin panel and the thermal protection system (TPS) was performed. The heated skin panel analyzed was rectangular in shape and contained a small square cool region at its center. The wing skin immediately outside the cool region was found to be close to the state of elastic instability in the chordwise direction based on the conservative temperature distribution. The wing skin was found to be quite stable in the spanwise direction. The potential wing skin thermal instability was not severe enough to tear apart the strain isolation pad (SIP) layer.

Also, the preflight thermal stress analysis was performed on the TPS tile under the most severe temperature gradient during the simulated reentry heating. The tensile thermal stress induced in the TPS tile was found to be much lower than the tensile strength of the TPS material. The thermal bending of the TPS tile was not severe enough to cause tearing of the SIP layer.

17. Key Words (Suggested by Author(s))	18. Distribution Statement
Orbiter wing skin SIP Thermal buckling Thermal stresses TPS	Unclassified — Unlimited Subject category 39

19. Security Classif. (of this report)	20. Security Classif. (of this page)	21. No. of Pages	22. Price*
Unclassified	Unclassified	22	A02

For sale by the National Technical Information Service, Springfield, Virginia 22161.